

Annealing behavior and electrical properties of atomic layer deposited PbTiO₃ and PZT films

Jung In Yang^{a,*}, Aaron Welsh^a, Nick M. Sbrockey^b, Gary S. Tompa^b, Ronald G. Polcawich^c, Daniel M. Potrepka^c, Susan Trolier-McKinstry^a

^a The Pennsylvania State University, University Park, PA 16802, United States

^b Structured Materials Industries, Inc., Piscataway, NJ 08854, United States

^c U.S. Army Research Laboratory, Adelphi, MD 20783, United States

ARTICLE INFO

Article history:

Available online 17 April 2018

Communicated by T. Paskova

Keywords:

A3. Atomic layer deposition

B1. Lead titanate (PbTiO₃)

B1. Lead zirconium titanate (PZT)

B2. Ferroelectric

B2. Piezoelectric material

ABSTRACT

The annealing behavior and electrical properties of lead titanate (PTO) and lead zirconate titanate (PZT) thin films deposited by atomic layer deposition (ALD) were investigated. ALD films were deposited on platinized silicon substrates. The composition of the PTO films ranged from Pb-deficient Pb_{0.73}TiO_{3-x} to Pb-rich Pb_{2.3}TiO_{3-x}, including stoichiometric PbTiO₃. The PZT films were all Pb-deficient, with Pb/(Zr + Ti) ratios of 0.40–0.75. Stoichiometric PbTiO₃ films showed the perovskite structure, and a well-defined, dense microstructure after crystallization at 600 °C for 1 min in 2 slpm O₂ in a rapid thermal annealer (RTA). Pb excess PbTiO₃ films developed into perovskite PbTiO₃ after annealing but the surface microstructure showed a large grained microstructure with significant porosity. The dielectric constant was 140 at 10 kHz and a ferroelectric polarization – electric field curve was observed. A Pb-deficient Pb_{0.66}Zr_{0.55}Ti_{0.45}O_{3-x} film showed a dense and fine-grained microstructure after annealing at 700 °C for 1 min in 2 slpm O₂ in a rapid thermal annealer (RTA). The dielectric constant was 100 at 10 kHz.

© 2018 Elsevier B.V. All rights reserved.

1. Introduction

Ferroelectric materials such as lead titanate (PbTiO₃) or lead zirconate titanate (Pb(Zr,Ti)O₃, PZT) have been researched intensively for microelectromechanical systems (MEMS) such as actuators, sensors, and energy harvesters due to the high piezoelectric and pyroelectric properties [1–3]. In many cases, the design of MEMS would benefit from 3-dimensional coatings of the piezoelectric layer. However most deposition techniques, including chemical solution deposition (CSD) [4], RF magnetron sputtering [5], and pulsed laser deposition (PLD) [6] are better suited to coating planar surfaces. In contrast, mist deposition [7] and metal-organic chemical vapor deposition (MOCVD) allow deposition over substantial topography [8,9]. Various modifications of MOCVD have been introduced, including plasma assisted MOCVD [10] and laser induced MOCVD [11]. However, atomic layer deposition (ALD) would permit superior conformality, and so would be of interest for this application.

Atomic layer deposition (ALD) is a chemical vapor deposition process that utilizes metal precursors and reactants at low

temperature. ALD is a surface controlled process due to alternate introduction of precursors and reactants. Ideally, each process step is self-limiting, enabling easy control of the thickness by the number of cycles of deposition [12–14]. The ALD method is known to provide outstanding uniformity and conformality in 3-dimensional structures in the case of binary oxides [15].

However, ALD deposition of ternary oxides, especially lead-containing materials, has several challenges, such as controlling the composition ratio accurately (especially the Pb concentration) [16,17]. Thus, PbTiO₃ and PZT thin films by ALD process have rarely been studied. Harjuoja et al. showed that perovskite PbTiO₃ thin films with excellent stoichiometry and uniformity could be grown by ALD after annealing at 600 °C in an oxygen atmosphere [18]. Hwang et al. reported that perovskite PbTiO₃ was obtained by ALD using Pb(DMAMP)₂ and Ti(OtBu)₄ as the Pb and Ti precursors respectively, and H₂O as the reactant at 200 °C. Amorphous as-grown films were crystallized between 500 °C and 600 °C [19].

Control of the PTO and PZT film composition in the as-deposited state was demonstrated in a separate study [20]. This research was focused on the relation between the film composition and the annealing conditions, with an emphasis on the crystallization behavior and electrical properties of ALD PbTiO₃ and PZT films.

* Corresponding author.

E-mail address: jxy194@psu.edu (J.I. Yang).

2. Experimental procedure

PbTiO₃ and PZT thin films were deposited on (1 1 1) platinized silicon wafers (Inostek 150 nm (1 1 1) Pt/20 nm TiO₂/300 nm SiO₂/(1 0 0) p-Si (~0.5 in X 1.0 in) by an ALD process with a one inch OD quartz tube. (NanoH-ALD™ tool, Structured Materials Industries, Inc. (SMI)). A detailed thin film growth process for PbTiO₃ and PZT by ALD was developed and reported on elsewhere [20]. Tetraethyl lead, Pb(Et)₄, tetrakis ethylmethylamino zirconium (TEMAZ) and tetrakis dimethylamino titanium (TDMAT) were employed as the Pb, Zr, Ti metal precursors, respectively. Ozone (O₃) was utilized as the oxidant of Pb(Et)₄ and either water or O₃ was used as the reactant of the TEMAZ or TDMAT precursors.

All films were annealed at various temperatures ranging from 550 °C to 700 °C and times from 1 to 16 min at 2 slpm O₂ flow in a rapid thermal annealer (RTA, All-win21 Corp AW 810). In the case of Pb excess PbTiO₃ films, the perovskite structure was observed at all temperatures. However, for films that were substantially Pb excess, the microstructure remained porous for higher annealing temperatures and time, as shown in Fig. 1. As a result, the annealing temperature was decreased to 550 °C or 600 °C for 1 min to measure the electrical properties.

X-ray diffraction (Panalytical X'pert Pro MPD) was used to characterize the phase of the PbTiO₃ and PZT thin films. The film composition was assessed either by energy-dispersive X-ray spectroscopy (EDS) in a FESEM (Nova Nano SEM 630, FEI Company) or by X-ray fluorescence (XRF, Amptek Eclipse II). Also, the Zr concentration in the films was measured by X-ray photoelectron spectroscopy (XPS). The film microstructure of films was characterized by a Zeiss Merlin field emission scanning electron microscope (Merlin FE-SEM).

For the electrical measurement, top platinum electrodes were patterned by a lift-off process to obtain 200 μm circular patterns on the films. First, LOR -5A photoresist (Microchem) was spun on films at 4000 rpm for 40 s and baked at 180 °C for 2 min. This was followed by spinning SPR 3012 photoresist on the LOR-5A layer at the same spin speed and baking at 95 °C for 1 min. The 1 μm thick 3012 photoresist (Dow Electronic Materials, Marlborough, MA) was exposed for 7 s using a contact mask aligner (MA/BA6, Suss Microtec) and then was developed in MF-CD 26 developer (Rohm and Haas Electronic Materials LLC, Marlborough, MA) for 1 min. Lastly, the sample was rinsed with flowing deionized water and an oxygen plasma ashing process (M4L, MetroLine) was performed to remove any residual resist on films. After the oxygen plasma ashing, a 100 nm thick platinum layer was deposited on the patterned film using RF sputtering (Kurt Lesker CMS-18 sputtering tool) with 200 W RF power with a 150 mm distance from target to substrate. After top Pt deposition, the patterned photoresist was lifted-off using acetone, 2-propanol and deionized

water. Finally, films were annealed at 550 °C for 1 min without O₂ gas flow in the RTA.

Baseline properties such as dielectric constant, loss tangents, and the Rayleigh parameters were characterized using a Hewlett-Packard 4284A LCR meter (Agilent Technology, Palo Alto, CA) at a

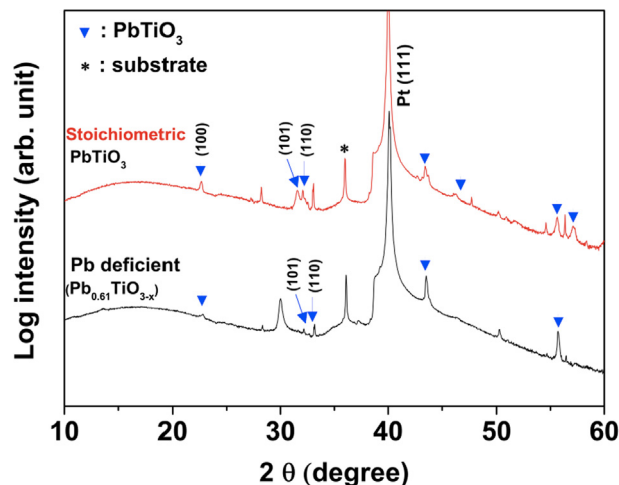


Fig. 2. XRD patterns of (a) Pb deficient PbTiO₃ thin film (Pb_{0.61}TiO_{3-x}) and (b) stoichiometric PbTiO₃ thin film annealed at 700 °C for 1 min.

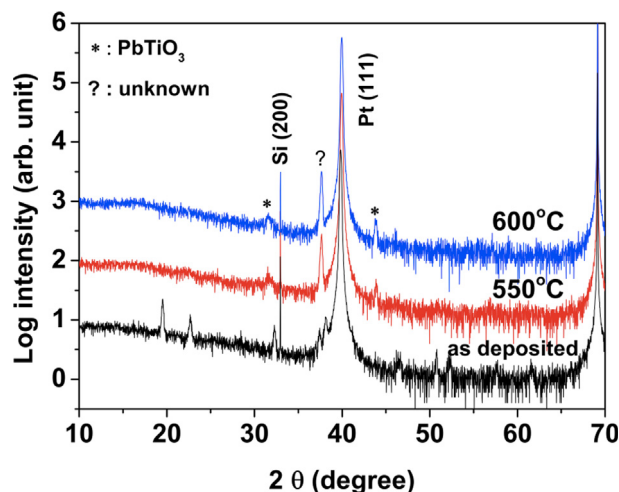


Fig. 3. XRD patterns of a 156 nm thick PbTiO₃ film after rapid thermal annealing at 550 °C and 600 °C.

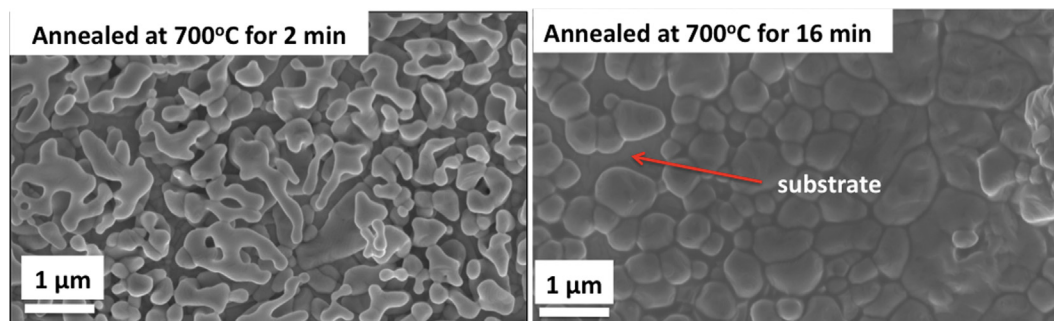


Fig. 1. FESEM surface images of PbTiO₃ films with substantially Pb rich compositions (Pb_{2.3}TiO_{3-x} film), where the relative cation composition has been normalized to a Ti content of one, annealed at (a) 700 °C for 1 min and (b) at 700 °C for 16 min at 2 slpm O₂ flow in RTA.

frequency of 10 kHz. Polarization – electric field (P–E) hysteresis loops were measured with an RT-66A Multi Ferroic Test System (Radiant Technology, Inc. Albuquerque, NM) at 100 Hz.

3. Results and discussion

The Pb, Zr and Ti composition and annealing temperature were varied to investigate the formation of the perovskite structure in the PbTiO_3 and PZT thin films. All films were amorphous in the as-deposited condition, as observed by X-ray diffraction. In this work, the range of Pb concentration $[\text{Pb}/(\text{Pb} + \text{Ti})]$ varied from 42.5 atomic% to 70 atomic%; the annealing temperature was varied from 550 °C to 700 °C. The RTA anneals were for 1 min in 2 slpm

oxygen flow with a ramp rate of 10 °C/s. It was found that it was imperative to heat treat the ALD samples after deposition at 350 °C for 5 min on a hot plate before the RTA step. This was needed to collapse the thickness prior to crystallization to minimize entrapped porosity or organics. Fig. 2 shows the X-ray diffraction patterns depending on the Pb composition (Pb deficient and Pb excess). It was found that perovskite PbTiO_3 developed from stoichiometric or Pb excess compositions on annealing at 700 °C. In contrast, strongly Pb deficient PbTiO_3 films did not show the perovskite phase at this annealing temperature; rather a pyrochlore phase developed on heat-treatment.

In this research, films with the composition $\text{Pb}_{0.98}\text{Ti}_{1.00}\text{O}_{3-x}$, which is stoichiometric within the error of the composition

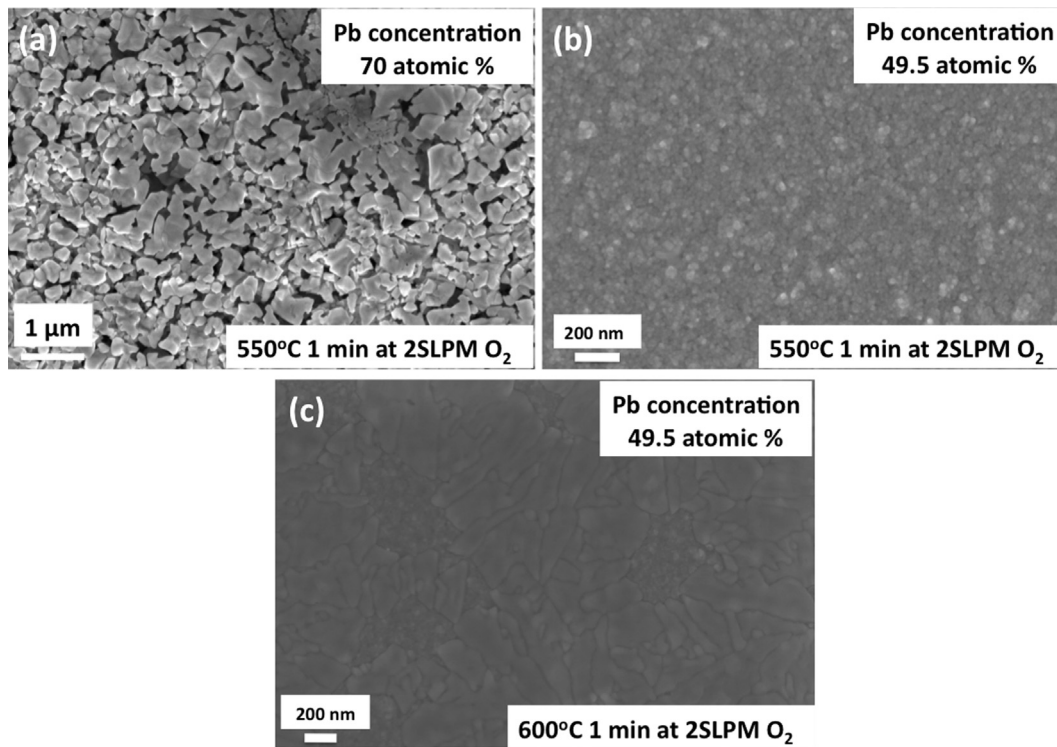


Fig. 4. FESEM surface images of (a) PbTiO_3 films with a Pb rich composition ($\text{Pb}_{2.3}\text{TiO}_{3-x}$ film), (b) and (c) stoichiometric composition annealed at 550 °C and 600 °C, respectively.

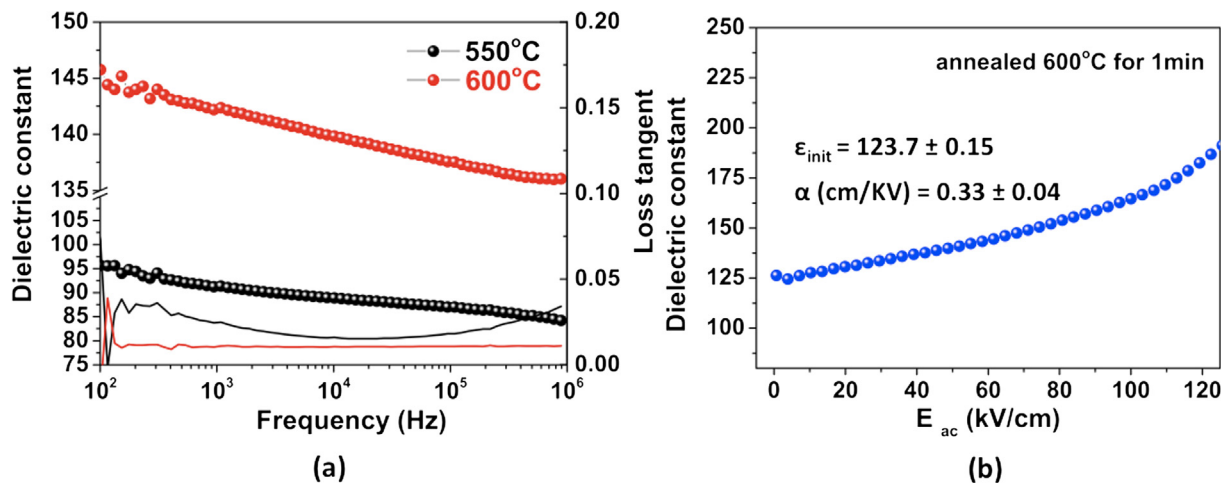


Fig. 5. (a) The frequency dependent dielectric constant and loss tangent of a 156 nm thick PbTiO_3 film annealed at 550 °C or 600 °C for 1 min at 2 slpm O_2 flow and (b) Rayleigh parameters of the film annealed at 600 °C for 1 min at 2 slpm O_2 flow.

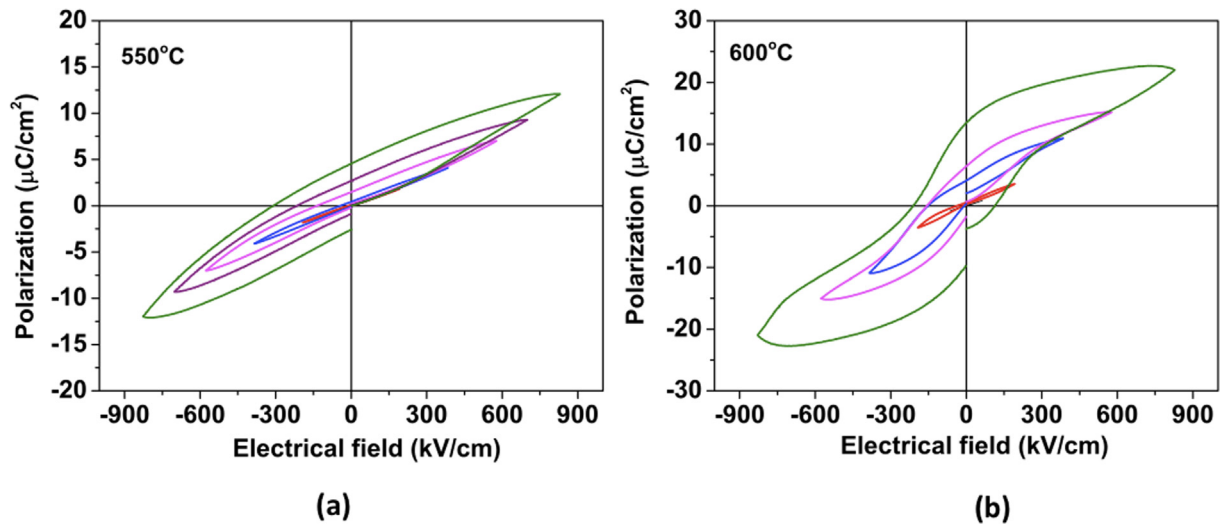


Fig. 6. P-E hysteresis loop measured at 100 Hz for a 156 nm thick PbTiO_3 film annealed at (a) 550 °C and (b) 600 °C for 1 min at 2 slpm O_2 flow in RTA.

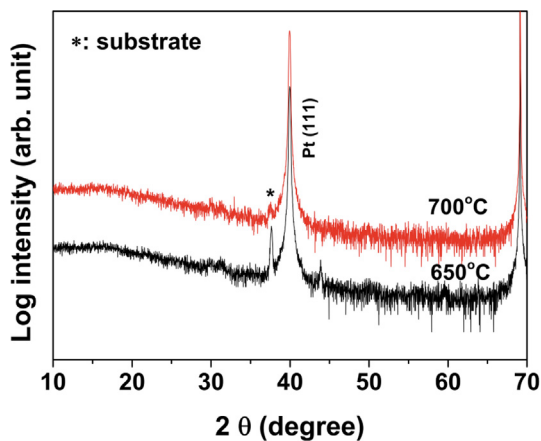


Fig. 7. XRD patterns of variations of annealing temperature at 650 °C and 700 °C for $\text{Pb}_{0.66}\text{Zr}_{0.55}\text{Ti}_{0.45}\text{O}_{3-x}$ film with 231 nm thickness.

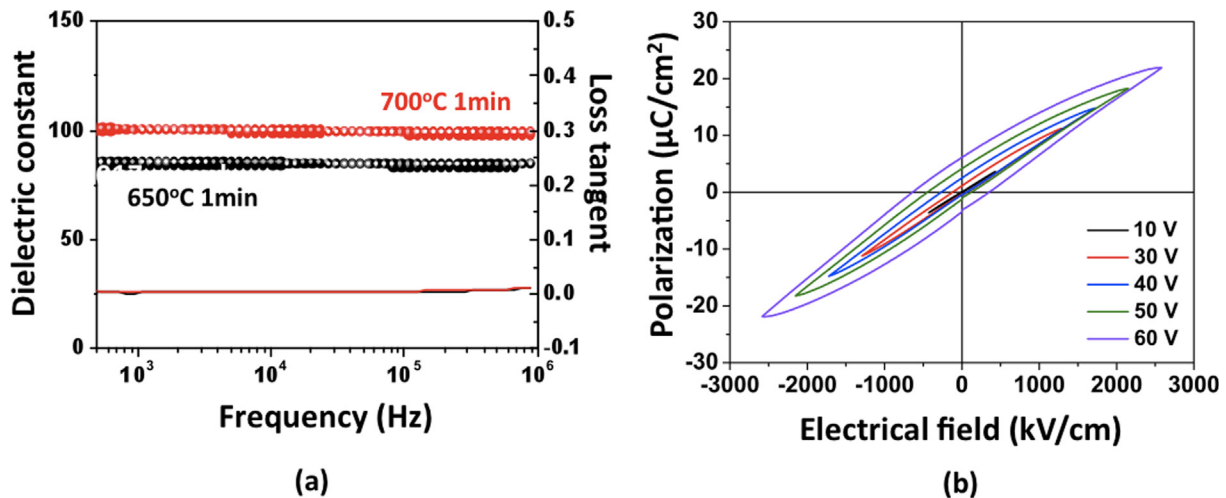


Fig. 8. (a) The frequency dependent dielectric constant and loss tangent and (b) P-E hysteresis loop measured at 100 Hz for a 231 nm thick $\text{Pb}_{0.66}\text{Zr}_{0.55}\text{Ti}_{0.45}\text{O}_{3-x}$ annealed at 650 °C for 1 min at 2 slpm O_2 flow in RTA.

measurements, showed the best results. Fig. 3 indicated that the stoichiometric PbTiO_3 ALD film was amorphous as-deposited. After annealing from 550 °C to 600 °C in the RTA, the perovskite structure was observed.

FESEM images were used to investigate the surface microstructure following annealing at various temperatures. Fig. 4 showed FESEM surface images of PbTiO_3 films with (a) Pb rich composition ($\text{Pb}_{2.3}\text{TiO}_{3-x}$ film), (b) and (c) with stoichiometric composition annealed at 550 °C and 600 °C, respectively. As shown in Fig. 4(a), the $\text{Pb}_{2.3}\text{TiO}_{3-x}$ films showed a large grained microstructure with significant porosity after annealing at 500 °C for 1 min at 2 slpm O_2 flow. In contrast, films with stoichiometric compositions showed less well-defined, but dense microstructures after crystallization under the same conditions (or at 600 °C, not shown).

The dielectric constant, dielectric loss, Rayleigh parameters and ferroelectric properties like polarization – electric field (P-E) hysteresis loops of the PbTiO_3 film were measured. All measurements were performed on films annealed at 550 °C or 600 °C for 1 min in 2 slpm O_2 flow in RTA. Fig. 5(a) showed the frequency dependence

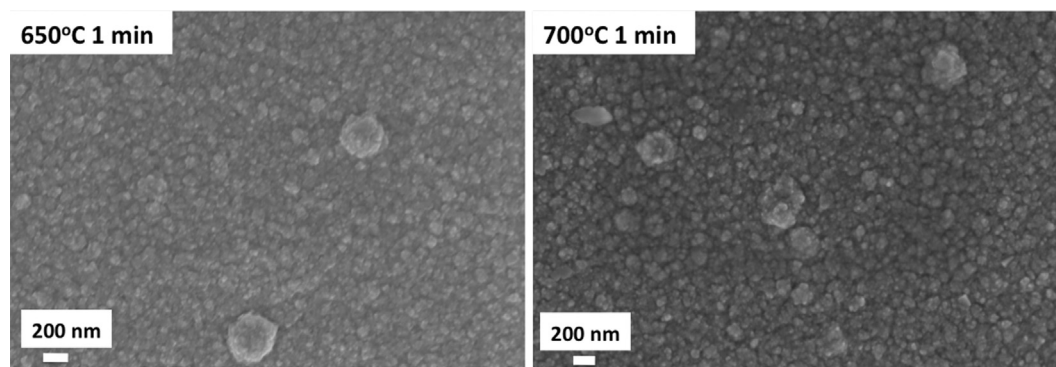


Fig. 9. FESEM surface images of $\text{Pb}_{0.66}\text{Zr}_{0.55}\text{Ti}_{0.45}\text{O}_{3-x}$ annealed at 650 °C or 700 °C for 1 min at 2 slpm O_2 flow in RTA.

of the dielectric constant and loss tangent for a 156 nm thick PbTiO_3 film measured at an oscillation voltage of 30 mV. The range of dielectric constant and the loss tangent was 88–95 and 0.015–0.3 for 550 °C annealed PbTiO_3 films and 136–145 and 0.01–0.02 for 600 °C annealed PbTiO_3 films from 10^2 to 10^6 Hz.

Fig. 5(b) illustrates the nonlinear dielectric response at low electric fields to assess whether the sample follows the Rayleigh law. It was observed a non-zero value for the irreversible Rayleigh coefficient α , which is associated with motion of domain walls, as shown in Fig. 5(b). This suggests that the films are in fact, ferroelectric, which would be consistent with the relatively high permittivity observed.

Fig. 6 shows polarization switching data for a 156 nm thick PbTiO_3 film annealed at 550 °C or 600 °C for 1 min. The data for the film annealed at 550 °C is consistent with a lossy capacitor, while a lossy ferroelectric loop is apparent for the 600 °C annealed PbTiO_3 film.

PZT films were grown by ALD over a range of Pb/Zr/Ti precursor ratios using similar experimental conditions as the PbTiO_3 films. In this work, $\text{Pb}_{0.66}\text{Zr}_{0.55}\text{Ti}_{0.45}\text{O}_{3-x}$ thin film (Pb deficient in terms of the Pb/(Zr + Ti) ratio) was used. The film was grown to 231 nm thickness. The as-deposited sample was heat treated at 350 °C for 5 min on the hot plate and then annealed at 650 °C or 700 °C for 1 min at 2 slpm O_2 flow in the RTA. The film crystallinity, microstructure and electrical properties were investigated. Figs. 7 and 8 showed the diffraction patterns, dielectric constant, loss tangent, and P-E hysteresis loop for $\text{Pb}_{0.66}\text{Zr}_{0.55}\text{Ti}_{0.45}\text{O}_{3-x}$ thin film. It is apparent that there is no evidence of the perovskite structure in the film. Fig. 9 showed FESEM images of $\text{Pb}_{0.66}\text{Zr}_{0.55}\text{Ti}_{0.45}\text{O}_{3-x}$ thin film annealed at 650 °C or 700 °C for 1 min respectively. A dense and fine grain microstructure was observed. Considerable optimization of the composition is required to demonstrate ferroelectricity in ALD PZT films.

4. Conclusions

The annealing behavior and electrical properties of PbTiO_3 and PZT thin films deposited by ALD using metal alkyl and metal amino type precursors were studied. It was found that the crystallization behavior and electrical properties of ALD PbTiO_3 and PZT films are highly dependent on both the film composition and the annealing conditions. All films were X-ray amorphous as deposited. Films with strongly lead-excess compositions ($\text{Pb}_{2.3}\text{TiO}_{3-x}$) crystallized well into the perovskite phase from 550 °C to 700 °C, however the resulting film exhibited a porous microstructure ostensibly due to loss of the excess PbO. Stoichiometric PbTiO_3 films showed well-defined dense microstructures after crystallization. The best results for stoichiometric PbTiO_3 films annealed at 600 °C showed

a dielectric constant of 140 and loss tangents of 0.01–0.02 at 10 kHz, with a lossy ferroelectric P-E curve. For a $\text{Pb}_{0.66}\text{Zr}_{0.55}\text{Ti}_{0.45}\text{O}_{3-x}$ film, little crystallinity was observed after annealing; the resulting film showed a dielectric constant of 100 at 10 kHz with a loss tangent of 0.01–0.04.

Acknowledgements

The authors thank the Army Research Office under STTR Phase II Contract Number W911NF-14-C-0163 for providing financial support for this research.

References

- [1] J.F. Scott, C.A. Paz de Araujo, Ferroelectric memories, *Science* 246 (1989) 1400.
- [2] P. Muralt, R.G. Polcawich, S. Troler-McKinstry, Piezoelectric thin films for sensors, actuators, and energy harvesting, *MRS Bull.* 34 (2009).
- [3] D. Dimos, S.J. Lockwood, R.W. Schwartz, Thin-film decoupling capacitors for multichip modules, *IEEE Trans. Compon. Packag. Manuf. Technol. Part A* 18 (1995) 174–179.
- [4] Robert W. Schwartz, Chemical solution deposition of perovskite thin films, *Chem. Mater.* 9 (11) (1997) 2325–2340.
- [5] K. Tsuchiya, T. Kitagawa, E. Nakamachi, Development of RF magnetron sputtering method to fabricate PZT thin film actuator, *Precision Eng.* 27 (3) (2003) 258–264.
- [6] Robert Eason, Pulsed Laser Deposition of Thin Films, Published by John Wiley & Sons, Inc., 2007.
- [7] M.D. Losego, S. Troler-McKinstry, Mist deposition of micron-thick lead zirconate titanate films, *Mat. Res. Soc. Symp. Proc. vol. 784*, C11.28, 2004, 1–6.
- [8] Warren C. Hendricks, Seshu B. Desu, Chien H. Peng, Metalorganic chemical vapor deposition of lead titanate, *Chem. Mater.* 6 (11) (1994) 1955–1960.
- [9] J.S. Zhao, H.J. Lee, J.S. Sim, K. Lee, C.S. Hwang, Ferroelectric and reliability properties of metal-organic chemical vapor deposited $\text{Pb}(\text{Zr}_{0.15}\text{Ti}_{0.85})\text{O}_3$ thin films grown in the self-regulation process window, *Appl. Phys. Lett.* 88 (17) (2006) 172904.
- [10] T. Mihara, S. Mochizuki, S. Kimura, R. Makabe, Relationship between crystal structure and chemical composition of PbTiO_3 thin films prepared by sputter-assisted plasma CVD, *Jpn. J. Appl. Phys. vol. 31, Part 1, No. 6A*, (1992), pp. 1872–1873.
- [11] K. Tokita, F. Okada, Growth of metal oxide thin films by laser-induced metalorganic chemical vapor deposition, *J. Appl. Phys.* 80 (1996) 7073–7083.
- [12] J. Harjuoja, Atomic Layer Deposition of Binary and Ternary Lead and Bismuth Oxide Thin Films, PhD. Thesis, Helsinki University of Technology, (2007).
- [13] T. Watanabe, S. Hoffmann-Eifert, C.S. Hwang, R. Waser, Liquid-injection atomic layer deposition of TiO_x and Pb-Ti-O films, *J. Electrochem. Soc.* 153 (9) (2006) F199.
- [14] H.J. Lee, M.H. Park, Y.-S. Min, G. Clavel, N. Pinna, C.S. Hwang, Unusual growth behavior of atomic layer deposited PbTiO_3 thin films using water and ozone as oxygen sources and their combination, *J. Phys. Chem. C* 114 (29) (2010) 12736.
- [15] T. Watanabe, S. Hoffmann-Eifert, C.S. Hwang, R. Waser, Growth behavior of atomic-layer-deposited $\text{Pb}(\text{Zr}, \text{Ti})_{0x}$ thin films on planar substrate and three-dimensional hole structures, *J. Electrochem. Soc.* 155 (11) (2008) D715.
- [16] T. Watanabe, S. Hoffmann-Eifert, F. Peter, S. Mi, C. Jia, C.S. Hwang, R. Waser, Liquid injection ALD of $\text{Pb}(\text{Zr}, \text{Ti})_{0x}$ thin films by a combination of self-regulating component oxide processes, *J. Electrochem. Soc.* 154 (12) (2007) G262.
- [17] F. Zhang, Y.-C. Perng, J.H. Choi, T. Wu, T.-K. Chung, G.P. Carman, C. Locke, S. Thomas, S.E. Saddow, J.P. Chang, Atomic layer deposition of $\text{Pb}(\text{Zr}, \text{Ti})_{0x}$ on 4H-SiC for metal-ferroelectric-insulator-semiconductor diodes, *J. Appl. Phys.* 109 (12) (2011) 124109.

- [18] J. Harjuoja, A. Kosola, M. Putkonen, L. Niinisto, Atomic layer deposition and post-deposition annealing of PbTiO_3 thin films, *Thin Solid Films* 496 (2006) 346.
- [19] G.W. Hwang, H.J. Lee, K. Lee, C.S. Hwang, Atomic layer deposition and electrical properties of PbTiO_3 thin films using metallorganic precursors and H_2O , *J. Electrochem. Soc.* 154 (3) (2007) G69.
- [20] Nick M. Sbrockey, Gary S. Tompa, Mark A. Fanton, Kathleen A. Trumbull, Robert Lavelle, David W. Snyder, Ronald G. Polcawich, Daniel M. Potrepka, Composition control and step coverage for ALD deposited PbTiO_3 and PZT thin films, Submitted to This Journal, 2017.